COMMUNICATIONS IN SCIENCE AND TECHNOLOGY
Homepage: cst.kipmi.or.id

Palm oil mill effluent (POME) precipitation using ammonium-intercalated clay coagulant

Satria Jaya Priatna[a], Yusuf Mathiinul Hakim[b], Muhammad Afif Alfarizi[c], Siti Sailah[d], Risfidian Mohadi[b,e,*]

[a]*Department of Soil Science, Faculty of Agriculture, Sriwijaya University, Indralaya 30862, Indonesia*
[b]*Graduate School of Mathematics and Natural Sciences, Faculty of Mathematics and Natural Sciences, Sriwijaya University, Palembang, 30139, Indonesia*
[c]*Department of Chemistry, Faculty of Mathematics and Natural Sciences, Sriwijaya University, Indralaya, 30862, Indonesia*
[d]*Department of Physics, Faculty of Mathematics and Natural Sciences, Sriwijaya University, Indralaya, 30862, Indonesia*
[e]*Magister Program of Material Science, Graduate School of Sriwijaya University, Palembang, 30139, Indonesia*

Article history:
Received: 18 November 2022 / Received in revised form: 17 January 2023 / Accepted: 16 February 2023

Abstract

Clay intercalation has been completed to improve coagulation ability using ammonium ions intercalant via multi-step intercalation. The intercalated clay was confirmed by Scanning Electron Microscope-Energy Dispersive Spectroscopy analysis of expanded lamellar and reduction impurities. Fourier Transform Infra-Red analysis confirmed the sharp and strong peak adsorption at 1448 cm^{-1} as ammonium (NH_4^+) bending vibration, and X-Ray Diffraction analysis confirmed the peak shifting to smaller 2θ at 10.08° as increasing basal spacing because of ammonium ion intercalated. The Palm Oil Mill Effluent (POME) coagulation was carried out using contact time and coagulant dose variations to determine the optimum conditions, reaching 45 minutes of coagulation and 0.4 g coagulant was used. Furthermore, the turbidity, free fatty acid, and total suspended solids were measured to reach the reduction values of 93%, 49.7%, and 73.7%, respectively. The reusable study of ammonium-intercalated clay confirmed the stability of the three cycles of coagulation used.

Keywords: Clay; Intercalation; ammonium ions; coagulation; palm oil mill effluent (POME)

1. Introduction

Oil extracted from the palm (*Elaeis Guineensis Jacq.*) is included as a vital commodity due to its users around the world. Indonesia is one of the largest countries producing palm oil and exporter of raw materials. The data of the Ministry of Agriculture of the Republic of Indonesia revealed that in 2015 there were 11.3 million hectares of palm plantations and it could produce up to 37.5 million tons of palm oil [1]. The palm oil industry has become an over-productive sector that impacts the country's financial balance. Secondary products also produce the massive palm oil production; one of the largest is palm oil mill effluent (POME), annually disposed of up to 50 million m^3 in Indonesia and Malaysia [2].

Visually POME is the brown viscous liquid categorized as non-toxic waste but generating the disturbing odors and containing various soluble materials that can impact environmental quality [2]. As reported in literature, POME acutely pollutes the water body for containing 25 mg/L of Biological Oxygen Demand (BOD), 50 mg/L of Chemical Oxygen Demand (COD), 8 mg/L of fat and oil, 20 mg/L of suspended solid, and 40 mg/L of total solid [3]. Therefore, it is not highly suggested to dispose the POME directly into the ecosystem as it can affect the soil and water bodies system, especially vegetation [4].

Several methods have recently been improved for oil-based waste treatment, such as Fenton oxidation, membrane separation, adsorption, flocculation, and coagulation [5,6]. Considering its effectiveness and general use, the coagulation has been selected to improve for being easily separated from the final product. Natural materials have become interesting to improve as the coagulant candidate, considering their non-toxic character and abundance in nature [7]. Clay is the best candidate for natural coagulant improvement due to the high potency of modification [8–10]. Recent work has observed the coagulation capacity of clay as a coagulant aid of Poly-Aluminum Chloride (PAC) to car wash waste with 90 % removal capacity [11]. The modified organo-clays as coagulant aid of alum removed the pesticide waste up to 82% [12]. However, there is a need for the updated work in using the clay-based material as an individual coagulant.

Clay and clays mineral have been popular for a long time in view of their wide range of applications. All clay-based materials based are abundant as their formation during the tecto-volcanic process spreads on Earth [13]. There are two general groups of clay minerals with specific features that are appropriate for contamination problems, those are swelling clay generally formed in the continental area, and non-swelling clay is generally formed in the oceanic area [14,15]. Based on the swelling character, clay is formed by the composition of 2:1 or the sandwich layers of octahedral alumina layer and covered by tetrahedral silica layers. This then can make it to have a high ability to absorb water as it contains varying exchangeable actions; thus, it causes the clay to have coagulant potency [8,16,17].

This study focused on the modification of West Java clay started with the first step of multi-step intercalation of sodium and then was exchanged by the ammonium intercalant. Ammonium is suitable for clay adaptation in organic pollutant

* Corresponding author.
Email: risfidian.mohadi@unsri.ac.id
https://doi.org/10.21924/cst.8.1.2023.1034

treatment by hydrophobic interaction and effectiveness in increasing the clay interlayer [18,19]. This application has brought innovation on the clay-modified application in specific palm oil waste management. The clay-intercalated was tested in the POME coagulation according to the turbidity, free fatty acid (FFA), and total suspended solid (TSS) reduction parameters. Furthermore, the coagulant was used in three coagulation cycles to determine the POME coagulation's stability structure and capacity.

2. Materials and Methods

2.1. Instrumentation and chemicals

The pure clay was imported from the West Java region, and the precursor chemicals with pure grade quality including sodium chloride (NaCl), ammonium chloride (NH_4Cl), sodium hydroxide (NaOH), hydrochloride acid (HCl), and ethanol 95% were purchased from Sigma-Aldrich. Meanwhile, phenolphthalein was purchased from Merck and the distilled water was purchased from Bratachem. The palm oil mill effluent (POME) was imported from the palm oil production outlet in Palembang, South Sumatera.

The instrumentation for supporting data was conducted to X-Ray Diffraction (XRD) Rigaku Mini-flex600 in the condition of scanning sample at a speed of 1 deg/min in the 2θ scan range of 10-90°, Fourier Transform Infra-Red (FTIR) Perkin-Elmer UATR Spectrum 2 with a scan range of 400 – 4000 cm^{-1}, Scanning Electron Microscope-Energy Dispersive Spectroscopy (SEM-EDS) JEOL JSM 6510-LA using scanning energy 20 kV and 20,000 magnifications, and Eutech TN-100 Turbidimeter.

2.2. Clay intercalation

Clay intercalation was conducted in the literature [20,21] with modification. The pure clay was intercalated by the multi-step incorporation of sodium followed by ammonium through the following steps: mixing a saturated NaCl solution (333 mL) with the clay (100 g) for 2 hours, and then diluting it with distilled water for 10 minutes ratio of 1:2 of clay mixture to distilled water. The clay was then filtrated and re-dissolved in the saturated NaCl solution (333 mL) for 2 hours. The clay residue was separated and washed three times with boiled distilled water. The precipitated clay was put into a furnace of 200°C for 12 hours and denoted as C-Na.

Ammonium intercalation was executed by mixing the C-Na (50 g) with a saturated NH_4Cl solution (165 mL) for 2 hours. The mixture was diluted using distilled water by a ratio of 1:2 of clay mixture to distilled water. The clay precipitate was filtrated and re-dissolved with saturated NH_4Cl solution (165 mL) for 120 minutes. The precipitate was filtrated and washed with boiled distilled water, before being put into a furnace at 200 ºC for 12 hours. This material was denoted as C-NH.

2.3. Determination of optimum condition

The optimum condition was configured by measuring the initial pH and turbidity of the pure POME. The optimum time was determined by mixing 0.1 g of clay-based coagulant with 10 mL of POME, and then was processed at the rapid stirring of 100 rpm in variation of times for 5, 10, 20, 30, 45, and 60 minutes. Moreover, the determination of coagulant doses was completed by varying the doses in a variation of 0.1, 0.2, 0.3, 0.4, 0.5, and 0.6 g of clay-based coagulant by an identic process of the previous step. The solution was aged for 5 minutes to precipitate the flocs. The final turbidity and pH were then measured.

2.4. Free fatty acids (FFA) analysis

The FFA analysis was measured using the National Standard of Indonesia number 7709-2012 (based on the titrimetric method). The process was initiated by preparing 5 g of POME before and after coagulation by 0.1, 0.2, 0.3, 0.4, and 0.5 g clay-based coagulant. Each sample was added with boiled ethanol 95% (50 mL) and phenolphthalein indicator (three drops). The mixture was titrated with the standardized NaOH solution. The NaOH solution used was measured as the FFA level calculation. The FFA reduction level was measured by the following Equation 1 in the percentage of [22]:

$$\%\ FFA = \frac{V_{NaOH} \times N_{NaOH} \times Mr_{Palmitic\ acid}}{m_{POME} \times 1000} \times 100\% \quad (1)$$

V_{NaOH} is denoted as the total NaOH solution used at titration (mL), $Mr_{palmic\ acid}$ is denoted as a mass relative to Palmitic acid chemical structure (g/mol), and m_{POME} is denoted as the total mass of POME solution used (g).

2.5. Total suspended solid (TSS) analysis

The TSS analysis was measured using the National Standard of Indonesia number 6989.3-2019 based on the gravimetry method. The solution of POME before and after coagulation with an optimum condition was filtrated in the sterile filter paper, followed by drying in the oven for 1 hour. The total weight of the sample filtrated was weighed. The TSS reduction was measured based on the following Equation 2:

$$C_{tss} = \frac{(W_1 - W_0) \times 1000}{V_{sample}} \quad (2)$$

W_1 and W_0 are denoted as total mass after and before coagulation, respectively (g), and V_{sample} is denoted as the volume of sample used (mL).

2.6. Reusable study

0.4 g clay-based coagulant was added to 10 mL of POME and rapidly stirred at 100 rpm for 45 minutes. After the precipitate separated, the turbidity was measured. The residue subsequently was separated, cleaned using distilled water and dried to be used at the next coagulation. The whole mechanism was conducted for three cycles to analyze the stability of the coagulant agent.

3. Results and Discussion

The characterization of morphology and particle composition was confirmed by SEM-EDS (see Figure 1). Pure clay was observed as a compact material and the intercalation

process expanded the lamellar structure of clay. The intercalation process triggered the tactoids disaggregation and reduce the impurities of Ti^{+} particles as proven in the SEM analysis in Figure 1(b) [23,24]. Table 1 describes the clay-based coagulant's detailed compositional analysis. According to the literature, the high-temperature treatment and the excess amount of intercalant in the solution have affected the structural transformation of the broadening layer and cation formation on the surface material [20].

Table 1. The EDS analysis of compositional structure of clay modified

Element	PC (% mass)	C-NH (% mass)
C	17.67	15.01
O	38.23	40.28
Na	0.17	1.94
Mg	1.35	0.69
Al	7.04	9.13
Si	23.2	25.26
K	0.76	3.25
Ca	6.99	2.82
Ti	0.89	0
Fe	3.7	1.62

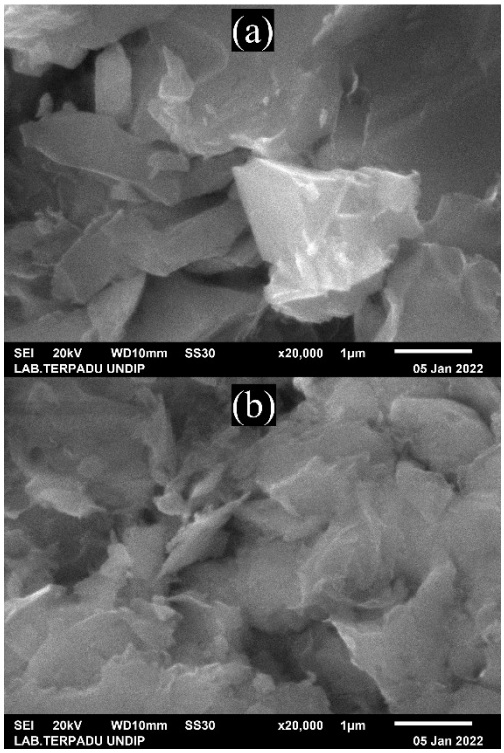

Fig. 1. SEM-EDS analysis of PC (a) and C-NH (b)

Furthermore, the transformation of functional group and bonding interaction was detected by FTIR analysis (Figure 2). The shifting of the transmittance band from 3626 to 3624 cm^{-1} and 3396 cm^{-1} indicated the slightly increasing vibration of the O-H group interlayer. The ammonium intercalant was detected by a higher intensity band at 1448 cm^{-1} as NH_4^{+} bending vibration and at 3253 cm^{-1} as NH_4^{+}-Si-OH stretching (this value was superimposed on the O-H stretching vibration) [25,26]. The high and sharp peak at 1005 cm^{-1} indicated the characteristic of silica tetrahedra vibration. Moreover, the triple difference of the band shown at 874 cm^{-1}, 796 cm^{-1}, and 518 cm^{-1} confirmed the alumina-silica octahedral.

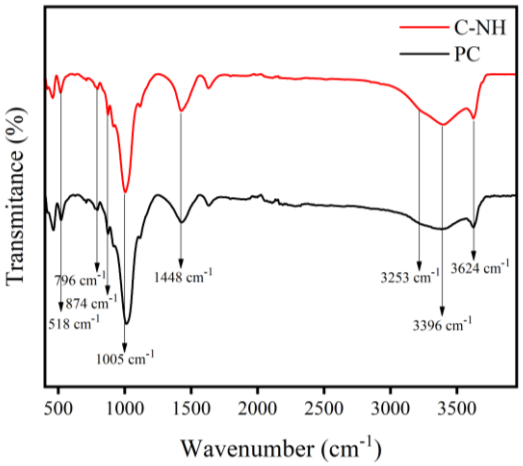

Fig. 2. FTIR spectrum of clay-intercalated coagulant

The XRD analysis determines the crystallinity transformation (see Figure 3(a)). The XRD orderliness of PC and C-NH showed some changes indicating the structural transformation. Based on the analysis, montmorillonite existing was indicated by the sharp and highest peak of 2θ at 20.08° and declared the dominant mineral in this West Java Clay structure. Kaolinite and quartz were noticed at 11° and 27.5°, respectively [27]. The kaolinite mineral disappeared after intercalation due to the disintegration between the detached platelet [28]. Moreover, the slight increase in quartz peak was affected by the re-structure of the intercalation process after calcination. Those were caused by the calcination process using 200°C of temperature [27,29–31]. According to Figure 3(b), the detailed diffractogram area between 10° and 11° strength proves interlayer lifting due to ammonium ion (NH_4^{+}) intercalation [32]. The ammonium ion had a bigger ionic radius (1.43Å) than the sodium ion (1.02Å); thus, affecting the expansion of layer distance [33].

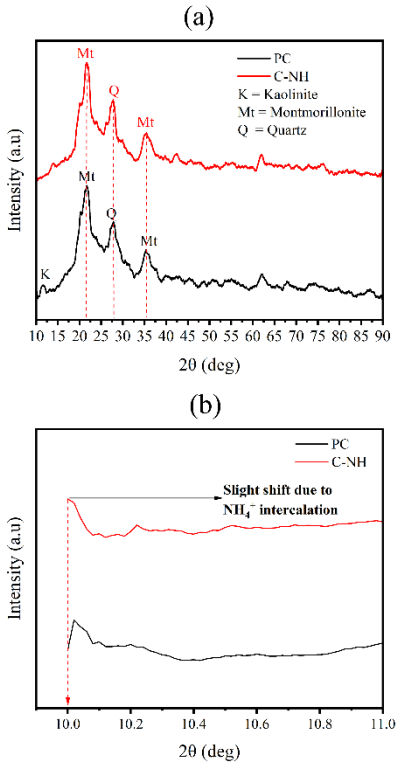

Fig. 3. XRD diffractogram of clay-modified coagulant (a) and the identification of ammonium intercalant in the diffractogram (b)

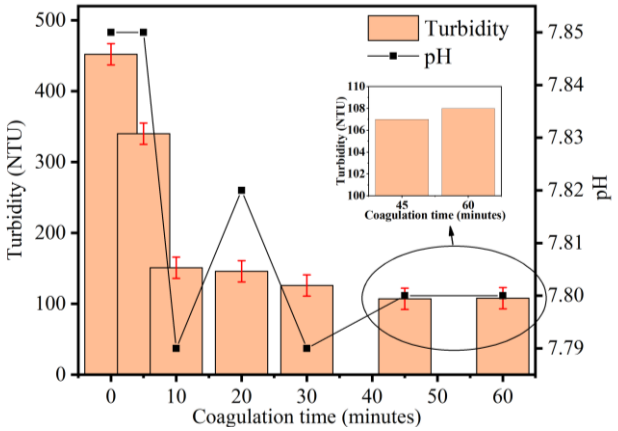

Fig. 4. The optimum coagulation time of POME using C-NH coagulant

An optimum condition observation was reached with varying coagulation times and coagulant doses. The optimum coagulation time was analyzed by determining the duration resulting from the highest turbidity reduction and the pH changes to understand the impact of clay-based coagulant (see Figure 4). As shown in Figure 4, the highest turbidity reduction reached pH 7.8 for 45 minutes of coagulation. The literature confirmed that clay-based coagulant is effective in the neutral pH range [34]. Furthermore, the optimum dose was reached with a ratio of 0.4 g/10 mL POME (see Figure 5). An anomaly on turbidity removal increased after the optimum dose due to the saturated capacity on neutralization and bridging of floc formation. Thus, the excess clay caused turbidity in the coagulation system [35].

Since determining the optimum condition parameter, the C-NH coagulant was used as the main coagulant in the next step of POME coagulation. The reduction of FFA and TSS was analyzed and shown in Figures 6 and 7, respectively. FFA reduction was included as an urgent parameter to avoid generating undesirable odors, hydrolysis, and triggering the oxidation process of the organic content of POME in the water bodies [36,37]. These processes became the reason eutrophication occurred. The decrease in FFA level meant the level reduction/precipitation of POME via neutralization by the structure charges of clay coagulant. A negative charge from the surface layer of clay and a positive charge from the ammonium intercalant can overcome the neutralization processes.

As shown in Figure 6, the optimum reduction of FFA levels

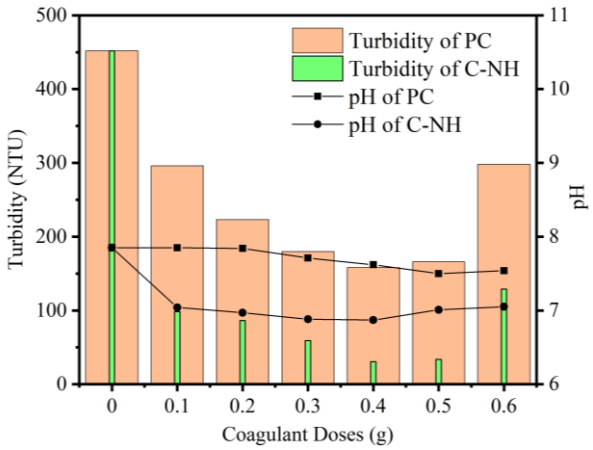

Fig. 5. The optimum coagulant doses on POME coagulation using clay-based Coagulant

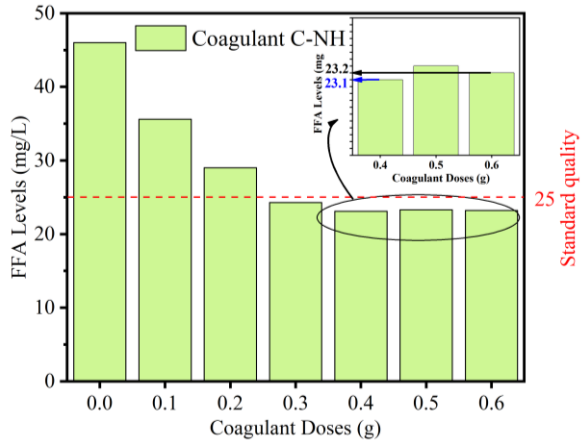

Fig. 6. The FFA reduction level in variation doses of C-NH coagulant

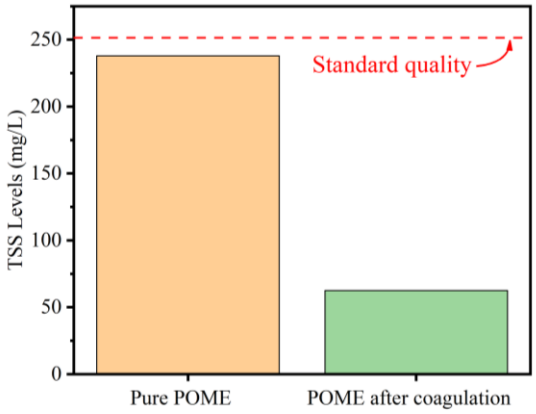

Fig. 7. The TSS reduction level of POME (before vs after coagulation)

after POME coagulation using C-NH reached 0.4 g doses. The increasing doses had no significant effect on FFA reduction with an assumption that the ammonium group can reach the saturated capacity in neutralization to form floc. The free fatty acid (palmitic acid) coagulation occurred when it interacted with the positive interlayer charges of NH_4^+ intercalant at a neutral pH range (at 7.8) hydrophobically and finely spread over the swelling interlayer clay materials [38]. The expected mechanism was figured out in Figure 9.

Data shown in Figure 7 compares the TSS level contained in the POME solution before and after coagulation (using 0.4 g doses of C-NH coagulant). The regulation of the State Minister of Environment Number 5/2014 about Wastewater Quality

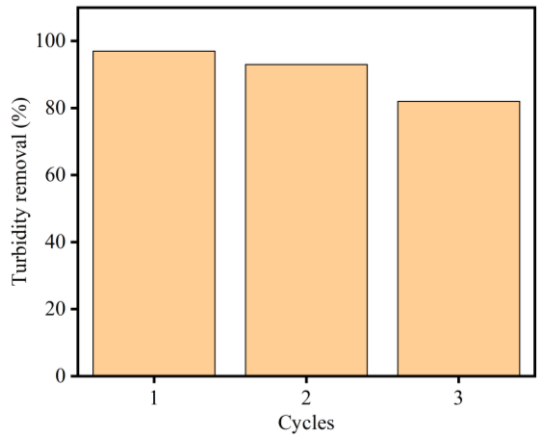

Fig. 8. The decreased turbidity value of POME along with three regeneration cycles

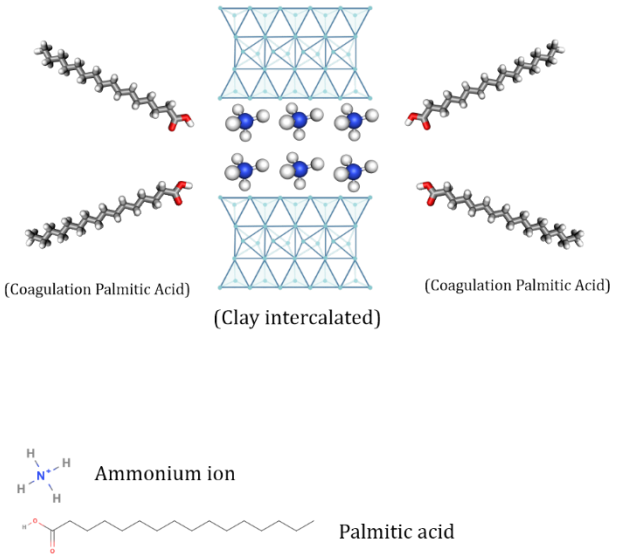

Fig. 9. The interaction mechanism of palmitic acid to clay-based coagulant

Standards, the final TSS levels of POME treated by clay-based coagulant fall under the standard quality. Furthermore, the regeneration trial has concluded that clay-based coagulant was effective up to three cycles application by the evidence of 83% turbidity reduction of the third cycle reusable as shown in Figure 8.

Table 2 describes the comparison of several coagulant abilities for POME removal. This work informed that the ammonium-intercalated clay performed appropriately in POME removal by coagulation. The proposed mechanism for this coagulation process was completed by neutralizing the POME charge by NH4+ groups, followed by bridging to flocculate due to the outstanding characteristic of clay as a precipitate agent [39,40].

Table 2. The comparison of coagulant agents used in POME removal

Coagulant agent	Additional Treatment	Reduction level	Ref.
Tanfloc from *Acacia mearnsii (plant)*	3 mg/L coagulant	40 % of TSS	[41]
Alum	The high temperature of 50 °C	86% of TSS	[42]
Peanut and Germ	1000.1 and 1170.5 mg/L coagulants, respectively	92.5 and 86.6 % (turbidity and TSS by peanut); 86.6 and 87.5 % (turbidity and TSS by germ)	[43]
Electro-coagulation	Assisted by H_2O_2	96.8% of TSS	[44]
Ammonium-intercalated Clay	Reached three cycles of reusability	49.7 % of FFA; 62.5 % of TSS; 93.2 % of turbidity	This work

4. Conclusion

The pure clay of the West Java area was intercalated using ammonium ions and confirmed by several analyses, including the SEM-EDS for the composition and swelling property changes, the FTIR for the functional group transformation, and the XRD for crystallinity changes. Moreover, this modified clay was found effective in flocculating the POME under the value regulated in Wastewater Quality Standards (Regulation of the State Minister of Environment Number 5/2014) by reduction of turbidity up to 93%, then FFA and TSS levels up to 23.1 mg/L (49.7%) and 62.5 mg/L (73.7%) 238 mg/L, respectively. The reusable process has proven that clay-intercalated has a stable structure to apply three cycles.

Acknowledgements

The authors acknowledge the instrumentation support by the Laboratory of Inorganic and Complex Materials and all of Prof. Risfidian Mohadi's research group members at the Magister Program of Material Science, Sriwijaya University.

References

1. E. Hambali and M. Rivai, *The Potential of Palm Oil Waste Biomass in Indonesia in 2020 and 2030*, IOP Conf Ser Earth Env. Sci., 65 (2017) 012050.
2. Statista Research Department, *Palm oil industry in Indonesia- statistics & facts*, Statista, (2023). https://www.statista.com/topics/5921/palm-oil-industry-in-indonesia/#topicOverview (accessed in Jan. 17, 2023).
3. C. Phalakornkule, J. Mangmeemak, K. Intrachod, and B. Nuntakumjorn, *Pretreatment of palm oil mill effluent by electrocoagulation and coagulation*, ScienceAsia, 36 (2010) 142.
4. Z. Othman, S. Bhatia, and A. Latif Ahmad, *Influence Of The Settleability Parameters For Palm Oil Mill Effluent (Pome) Pretreatment By Using Moringa Oleifera Seeds As An Environmental Friendly Coagulant.*, Inter. Conf. on Env. 2008 (ICENV 2008), (2014).
5. A. Mohammad, K. Ahmad, R. Rajak, and S. M. Mobin, *Remediation of Water Contaminants*, in Handbook of Ecomaterials, Cham: Springer Int. Pub., (2019) 373–391.
6. D. R. Wicakso, A. Mirwan, E. Agustin, N. F. Nopembriani, I. Firdaus, and M. Fadillah, *Potential of silica from water treatment sludge modified with chitosan for Pb(II) and color adsorption in sasirangan waste solution*, Commun. Sci. Technol., 7 (2022) 188–193.
7. D. Borah, H. Nath, and H. Saikia, *Modification of bentonite clay & its applications: a review*, Reiews. in Inorg. Chem., 42 (2022) 265–282.
8. M. Ahari, H. Ddahim, and R. Ramadane, *Performance of bentonite clay as a coagulation aid on water quality*, Desalination Water Treat., 143 (2019) 229–234.
9. S. J. Priatna, Y. M. Hakim, S. Wibyan, S. Sailah, and R. Mohadi, *Interlayer Modification of West Java Natural Bentonite as Hazardous Dye Rhodamine B Adsorption*, Sci. and Tech. Ind., 8 (2023) 160–169.
10. R. Mohadi, Y. M. Hakim, R. D. Astuti, I. Royani, and M. Mardiyanto, *Pillarization of Sumatera Bentonite by Sodium-assisted As Effective Adsorbent of Anionic Surfactants Sodium Lauryl Sulphate (SLS) Waste*, Bull. of Chem. Reaction Engineering & Catalysis, 18 (2023) 48–58.
11. G. Veréb, V. Gayýr, E. Santos, Fazekas, S. Kertész, C. Hodúr et al., *Purification of real car wash wastewater with complex coagulation/flocculation methods using polyaluminum chloride, polyelectrolyte, clay mineral and cationic surfactant*, Water Sci. and Tech., 80 (2020) 1902–1909.
12. T. P. A. Shabeer, A. Saha, V. T. Gajbhiye, S. Gupta, K. M. Manjaiah, and E. Varghese, *Simultaneous removal of multiple pesticides from water: Effect of organically modified clays as coagulant aid and adsorbent in*

coagulation–flocculation process, Environ. Tech., 35 (2014) 2619–2627.
13. M. J. Wilson, *The origin and formation of clay minerals in soils: past, present and future perspectives*, Clay Miner., (1999).
14. N. K. Foley, *Environmental Characteristics of Clays and Clay Mineral Deposits*, USGS, https://pubs.usgs.gov/info/clays/ (accessed Nov. 17, 2022) (2009).
15. Y. Wan, D. Guo, X. Hui, L. Liu, and Y. Yao, *Studies on Hydration Swelling and Bound Water Type of Sodium- and Polymer-Modified Calcium Bentonite*, Adv. in Polymer Tech., 2020 (2020) 1–11.
16. S. Farrokhpay, B. Ndlovu, and D. Bradshaw, *Behaviour of swelling clays versus non-swelling clays in flotation*, Miner. Eng., 96–97 (2016) 59–66.
17. Y. F. Arifin, M. Arsyad, J. Monica, and S. S. Agus, *Volume change in compacted claystone-bentonite mixtures as affected by the swamp acidic water*, Commun. Sci. Technol., 6 (2021) 80–90.
18. C. Gallo, P. Rizzo, and G. Guerra, *Intercalation compounds of a smectite clay with an ammonium salt biocide and their possible use for conservation of cultural heritage,* Heliyon, 5 (2019).
19. L. Xu, Y. Zhang, J. Zheng, H. Jiang, T. Hu, and C. Meng, *Ammonium ion intercalated hydrated vanadium pentoxide for advanced aqueous rechargeable Zn-ion batteries*, Mater. Today Energy, 18 (2020).
20. M. Laipan, L. Xiang, J. Yu, B.R. Martin, R. Zhu, J. Zhu et al., *Layered intercalation compounds: Mechanisms, new methodologies, and advanced applications*, Prog. Mater. Sci., 109 (2020) 1–97.
21. S. Lubis, *Preparasi Bentonit Terpilar Alumina dari Bentonit Alam dan Pemanfaatannya sebagai Katalis pada Reaksi Dehidrasi Etanol, 1-Propanol serta 2-Propanol*, J. Rek. Kim. dan Ling., 6 (2007) 77–81.
22. R. Luthfian Ramadhan Silalahi, D. Puspita Sari, and I. Atsari Dewi, *Testing of Free Fatty Acid (FFA) and Colour for Controlling the Quality of Cooking Oil Produced by PT. XYZ*, Industria: J. Tek. dan Man. Agro., 6 (2017) 41–50.
23. M. Sirait, N. Bukit, and N. Siregar, *Preparation and characterization of natural bentonite in to nanoparticles by co-precipitation method*, (2017) 020006.
24. J. Y. de Morais Pinos, L. B. de Melo, S. D. de Souza, L. Marçal, and E. H. de Faria, *Bentonite functionalized with amine groups by the sol-gel route as efficient adsorbent of rhodamine-B and nickel (II)*, Appl. Clay Sci., 223 (2022) 106494.
25. J. Pironon, M. Pelletier, P. de Donato, and R. Mosser-Ruck, *Characterization of smectite and illite by FTIR spectroscopy of interlayer NH 4 + cations*, Clay Miner., 38 (2003) 201–211.
26. Ali. E. I. Elkhalifah, S. Maitra, M. A. Bustam, and T. Murugesan, *Effects of exchanged ammonium cations on structure characteristics and CO2 adsorption capacities of bentonite clay*, Appl. Clay Sci., 83–84 (2013) 391–398.
27. L. Zhirong, Md. Azhar Uddin, and S. Zhanxue, *FT-IR and XRD analysis of natural Na-bentonite and Cu(II)-loaded Na-bentonite*, Spectrochim Acta A Mol Biomol Spectrosc., 79 (2011) 1013–1016.
28. R. L. Frost and J. Kristof, *Raman and Infra-Red Spectroscopic Studies of Kaolinite Surfaces Modified by Intercalation*, (2004).
29. E. Ringdalen, *Changes in Quartz during Heating and the Possible Effects on Si Production*, JOM, 67 (2015) 484–492.
30. Y. Hakim, R. Mohadi, M. Mardiyanto, and I. Royani, *Ammonium-Assisted Intercalation of Java Bentonite as Effective of Cationic Dye Removal*, J. of Ecological Eng., 24 (2023) 184–195.
31. Salah, Gaber, and Kandil, *The Removal of Uranium and Thorium from Their Aqueous Solutions by 8-Hydroxyquinoline Immobilized Bentonite*, Minerals, 9 (2019) 626.
32. L. A. Pérez-Maqueda, *Study of Natural and Ion Exchanged Vermiculite By Emanation Thermal Analysis, TG, DTA, and XRD,* J. Therm. Anal. Calorim., 71 (2003) 715–726.
33. H. Lindgreen, *Ammonium fixation during illite-smectite diagenesis in Upper Jurassic shale, North Sea*, Clay Miner., 29 (1994) 527–537.
34. S. Syafalni, I. Abustan, S. N. F. Zakaria, M. H. Zawawi, and R. A. Rahim, *Raw water treatment using bentonite-chitosan as a coagulant*, Water Sci. Tech. Water Supply, 12 (2012) 480–488.
35. D. I. M. Al-Risheq, S. M. R. Shaikh, M. S. Nasser, F. Almomani, I. A. Hussein, and M. K. Hassan, *Enhancing the flocculation of stable bentonite suspension using hybrid system of polyelectrolytes and NADES*, Colloids Surf. A Physicochem Eng. Asp., 638 (2022) 128305.
36. C. Vaisali, S. Charanyaa, P. D. Belur, and I. Regupathi, *Refining of edible oils: a critical appraisal of current and potential technologies*, Int. J. Food Sci. Tech., 50 (2015) 13–23.
37. K. Essid, M. Chtourou, M. Trabelsi, and M. H. Frikha, *Influence of the Neutralization Step on the Oxidative and Thermal Stability of Acid Olive Oil*, J. Oleo Sci., 58 (2009) 339–346.
38. B. Keskinler, A. Tanrizeven, N. Dizge, and E. Pakdemirli, *A Process For Removal of Free Fatty Acids From Vegetable Oils*, Google Patents WO2008140432A1 (2008)
39. Q. Wei, F. O. Mcyotto, C. W. K. Chow, Z. Nadeem, Z. Li, and J. Liu, *Eco-friendly decolorization of cationic dyes by coagulation using natural coagulant Bentonite and biodegradable flocculant Sodium Alginate*, SDRP J. of Earth Sci. & Env. Stud., 5 (2020) 51–60.
40. M. Czemierska, A. Szcześ, and A. Jarosz-Wilkołazka, *Purification of wastewater by natural flocculants*, BioTechnologia, 4 (2015) 272–278.
41. Z. Z. Abidin and M. A. Issa, *Coagulation Treatment of Palm Oil Mill Effluent Using Plant-Based Tannin*, Pollution Research, 37 (2018) 788–793.
42. S. Ismail, I. Idris, Y. T. Ng, and A. L. Ahmad, *Coagulation of Palm Oil Mill Effluent (POME) at High Temperature*, J. Applied Sci., 14 (2014) 1351–1354.
43. C. Y. Chung, A. Selvarajoo, V. Sethu, A. K. Koyande, A. Arputhan, and Z. C. Lim, *Treatment of palm oil mill effluent (POME) by coagulation flocculation process using peanut–okra and wheat germ–okra*, Clean Tech. Env. Policy, 20 (2018) 1951–1970.
44. M. JK. Bashir, J. H. Lim, S. S. Abu Amr, L. P. Wong, and Y. L. Sim, *Post treatment of palm oil mill effluent using electro-coagulation-peroxidation (ECP) technique*, J. Clean Prod., 208 (2019) 716–727.